The Structure of Platinum-Tin Reforming Catalysts

By R. Srinivasan and Burtron H. Davis
Center for Applied Energy Research, University of Kentucky, Lexington, U.S.A.

Platinum-tin on alumina catalysts appear to have potential for use during naphtha reforming in processes utilising continuous catalyst regeneration, and without the need for complex activation procedures. To gain a better understanding of the properties that contribute to their effectiveness, the surface and bulk characteristics of these bimetallic catalysts have been studied by a variety of techniques which make more direct measures of the chemical and physical states of the elements present than, for example, temperature-programmed reduction. The data presented demonstrate that catalyst formation by the addition of platinum and tin by co-precipitation leads to alloy formation, but that this does not occur when a support prepared by co-precipitating tin and aluminium oxide is impregnated with chloroplatinic acid.

The introduction of the bifunctional platinum/alumina catalyst for naphtha reforming shortly after the end of World War II led to a revolution in petroleum processing (1). On the commercial side, the reforming process provided a means of meeting the dramatic increase required in octane rating for gasoline, to provide an abundant source of aromatics for the rapidly developing petrochemicals industry, and to provide surplus hydrogen and so permit the development of other processes such as hydrotreating and hydrocracking. On the scientific side, the studies needed to define the mechanisms underlying the effectiveness of this bifunctional catalyst led to significant advances in the understanding of catalysis as well as of the reforming process.

While the platinum/alumina catalysts were an outstanding success, they had to be regenerated at rather frequent intervals: every three months or so. Thus, the introduction in the late 1960s of a platinum-rhenium bimetallic catalyst that could remain on-stream for a period of a year or even longer led to a second revolution in naphtha reforming (2). The platinum-rhenium/alumina catalyst had to be activated and brought on stream using a rather lengthy procedure which usually involved poisoning the catalyst with sulphur during a break-in period. Today, with the potential for a naphtha reforming process incorporating continuous catalyst regeneration, other bimetallic catalysts which do not require complex activation procedures must be utilised; platinum-tin/alumina appears to be an attractive catalyst for this process.

The reasons for the superior catalytic properties of these bimetallic catalysts are not fully understood even after 30 years of active research. Many of the explanations for the superior properties of the bimetallic catalysts are based on a structural point of view. Many argue that the bimetallic components form an alloy which has better catalytic properties than platinum alone. For example, alloy formation could influence the *d*-band electron concentration, thereby controlling selectivity and activity (3). On the other hand, the superior activity and selectivity may be the result of high dispersion of the active platinum component, and the stabilisation of the dispersed phase by the second component (4). Thus, much effort has been expended in order to define the extent to which metallic alloys are formed (for example, see References 5–18). These studies have

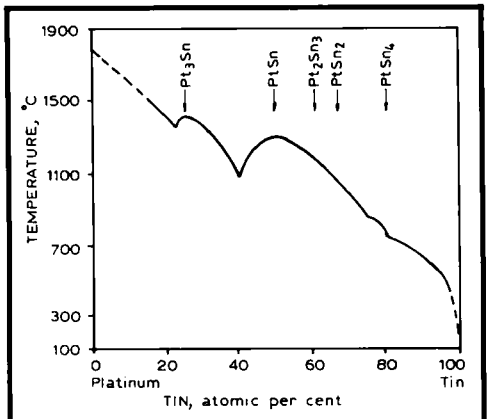

Fig. 1 Phase diagram of platinum-tin (19); with increasing tin:platinum, a series of alloys with increasing tin content form

utilised a variety of experimental techniques.

Platinum and tin present a complex situation since a number of alloy compositions are possible, depending upon the tin to platinum ratio. The phase diagram in Figure 1 shows that as the tin to platinum ratio increases it should be possible to form a series of alloys with increasing tin fractions (19, 20).

Temperature-programmed reduction (TPR), one of the indirect analysis methods, yielded data which suggested that tin was not reduced to the zero-valent state (10, 16). Burch has reviewed early work on the characterisation of this type of catalyst in an earlier issue of this journal (15). Based on results obtained from TPR studies, Lieske and Völter reported that a minor part of the tin is reduced to metal, and that this tin(0) combined with platinum to form "alloy clusters", but that the major portion of the tin is reduced to only the tin(II) state (21). They also reported that the amount of alloyed tin increases with increasing tin content.

In the following text, we report data from methods which make a more direct measure of the chemical or physical state of the platinum and/or tin present in platinum-tin/alumina catalysts; but because of space limitations this review outlines results primarily from our laboratory.

X-ray photoelectron spectroscopy (XPS) studies allow determination of the chemical state of an element but the data do not permit one to define whether tin(0), if present, is in the form of a platinum-tin alloy. Furthermore, the major platinum XPS peak coincides with a large peak from the alumina support. Thus, XPS can only provide data to indicate whether an alloy is possible; it cannot be used to prove the presence of a platinum-tin alloy.

The early XPS studies, including those from our laboratory, revealed that the tin is present only in an oxidised state (10, 16). These results were consistent with those for platinum-rhenium bimetallic catalysts where only oxidised rhenium was observed (9, 22). The early XPS data, at least from our laboratory, were apparently affected by the use of oxygen-containing pump oils to maintain the high vacuum needed for the operation of the XPS instrument. Thus, Li and co-workers reported that a portion of the tin in platinum-tin/alumina catalysts was present in the zero valence state (23); furthermore, it appears that the atomic ratio of the platinum-tin alloy, based upon the amount of platinum and tin(0) detected by XPS, increases with increasing ratios of tin to platinum. Typical spectra for the tin $3d_{5/2}$, $3d_{3/2}$ regions of a reduced catalyst having a platinum:tin composition of 1:8 (all catalysts contained 1 weight per cent platinum) are shown in Figure 2 (24). The spectrum for platinum in Figure 3 has been corrected for sample charging by using an aluminium $2p$ peak position of 74.7 eV. A small peak at approximately 480 eV is due to a small amount of tin that is present on the palladium sample holder. This small peak and the palladium peaks of the sample holder do not experience charging; this small tin peak is at a position indicative of metallic tin (or tin oxide in the oxidised sample) prior to correction for charging.

The spectra for the aluminium $2p$ and the platinum $4f$ regions are shown in Figure 3 for the same platinum to tin ratio of 1:8 sample. Because the aluminium $2p$ peak of the alumina support overlaps with the platinum $4f$ peaks, curve deconvolution was carefully carried out assuming the intensity ratio of $4f_{5/2}$ to $4f_{7/2}$

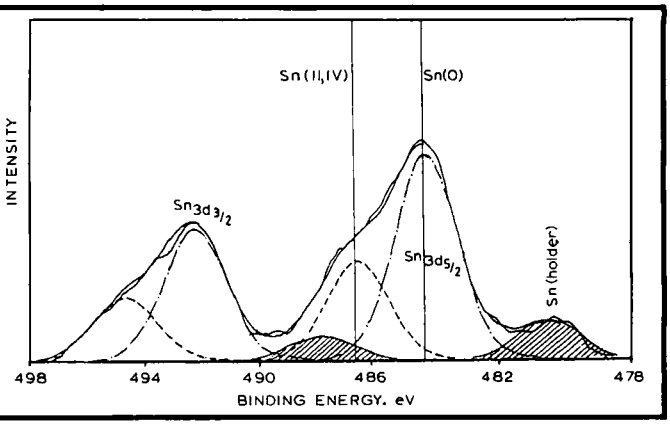

Fig. 2 XPS spectrum of the Sn_{3d} region for the reduced Pt-Sn/Al_2O_3 (250 m^2/g) catalyst with a Pt:Sn ratio of 1:8

was 0.75:1.0. The binding energies of the platinum peaks in Figure 3 are consistent with platinum being present as platinum(0). In this study three catalyst series were analysed using XPS. The compositions of the platinum-tin alloys (calculated by assuming all the platinum and the fraction of tin present as tin(0) formed an alloy) that are present in each catalyst of the three series are summarised in Table I. It appears that the alloy present contains increasing platinum:tin ratios as the ratio of platinum to tin on the catalyst is increased. However, XPS provides a measure of the surface, and not the bulk, composition; Bouwman and Biloen showed that tin is concentrated in the surface of a reduced sample of unsupported platinum-tin alloy (25). Our XPS results are in general agreement with those obtained in the extensive investigations by Hoflund and co-workers (26–32).

Stencel and co-workers utilised XPS together with scanning electron microscopy (SEM) to follow the interaction and migration of chlorine in platinum, rhodium and platinum-tin-containing catalysts (33). In situ reduction with hydrogen decreased the surface concentration of chloride, presumably by increasing the bulk chloride concentration. Subsequent oxygen treatment of these reduced catalysts caused the surface concentration of chloride to increase. In the case of rhodium/alumina, the characteristics of the aluminium *2p* peak after

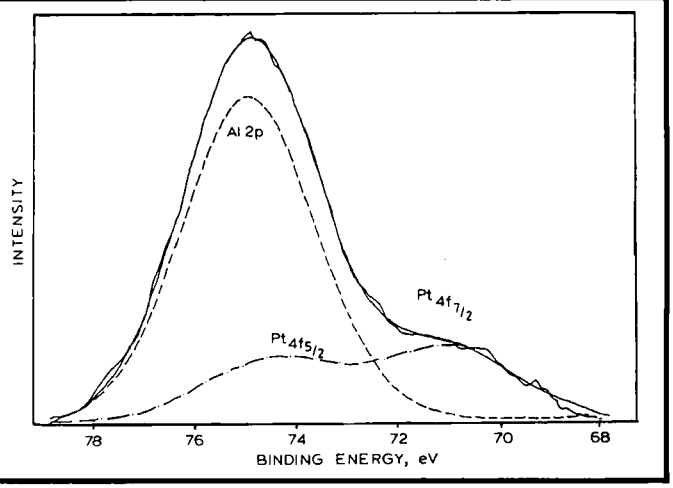

Fig. 3 XPS spectrum of the Pt_{4f} region for reduced Pt-Sn/Al_2O_3 (250 m^2/g) catalyst with a Pt:Sn ratio of 1:8

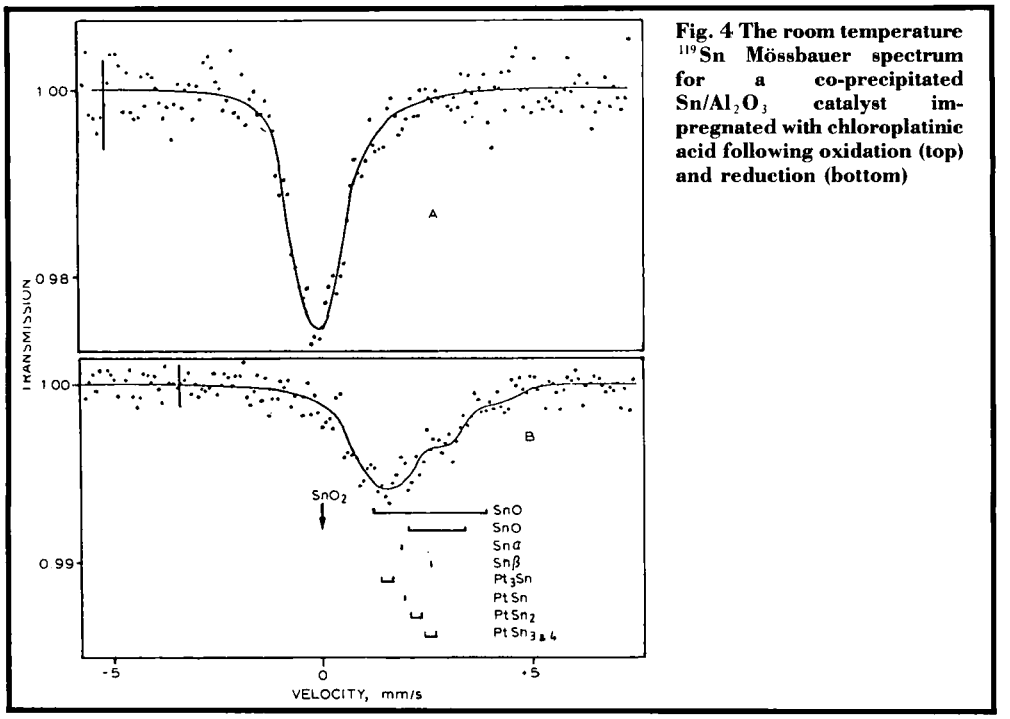

Fig. 4 The room temperature ^{119}Sn Mössbauer spectrum for a co-precipitated Sn/Al_2O_3 catalyst impregnated with chloroplatinic acid following oxidation (top) and reduction (bottom)

hydrogen reduction suggest the formation of $AlCl_3$-type species.

^{119}Sn Mössbauer data also provide a bulk diagnostic technique which has been utilised in a number of studies (for example, 7, 34–47). Direct evidence for platinum-tin alloy formation was obtained from Mössbauer studies (for example, 7, 42, 43, 46, 47); however, many of these studies were at high metal loadings and even then such a complex spectrum was obtained that there was some uncertainty in assigning tin(0) to the exclusion of tin oxide phases.

Table I

Pt-Sn Alloy Compositions Based upon XPS Data

	Support		
Pt:Sn	Alumina, 250 m²/g	Alumina, 110 m²/g	Silica
1:1	$PtSn_{0.66}$	$PtSn_{0.65}$	$PtSn_{0.39}$
1:2.7	$PtSn_{1.3}$	$PtSn_{1.3}$	$PtSn_{0.85}$
1:5	$PtSn_{3.4}$	$PtSn_{3.3}$	$PtSn_{1.5}$
1:8	$PtSn_{3.8}$	$PtSn_{2.6}$	

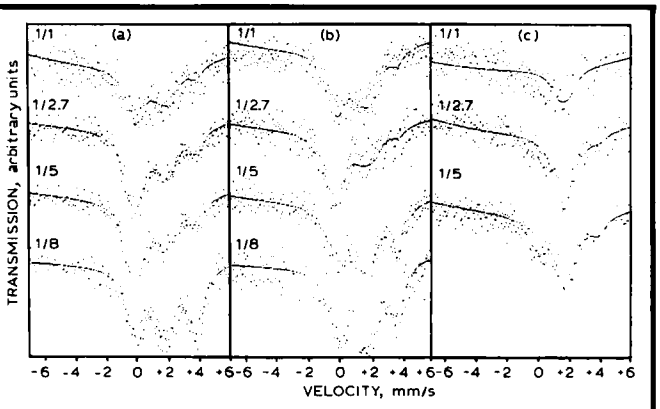

Fig. 5 ^{119}Sn Mössbauer spectra for reduced Pt-Sn catalysts: (a) Pt-Sn/Al_2O_3 (250 m^2/g), (b) Pt-Sn/Al_2O_3 (110 m^2/g), and (c) Pt-Sn/SiO_2 (700 m^2/g). (Pt:Sn mole ratios are indicated by the numbers shown in the Figure)

Mössbauer results clearly show changes upon reduction in hydrogen, but the width of the peaks for the reduced sample prevents, in general, a specific assignment for some states of tin. This is exemplified by the results of Kuznetsov and co-workers, who reported that platinum-tin/γ-alumina catalysts prepared by conventional impregnation techniques are multicomponent (42); that is, they have highly dispersed species that are a result of chemical interactions of tin(IV), tin(II), and tin(0) with both the support surface and the platinum. According to these authors, platinum forms nearly all possible alloys with tin. Examples of Mössbauer spectra and the isomer shifts associated with particular compounds or alloys are presented in Figure 4 (35).

The same series of catalysts that had been used earlier in their XPS studies (23) was utilised by Li and co-workers (48); each sample in the three series contained 1 weight per cent platinum and a varying amount of tin. Tin was observed to be present in forms whose isomer shifts were similar to or the same as those of SnO_2, SnO, $SnCl_4$, $SnCl_2$, tin(0) and platinum-tin alloy, when alumina was the support. Representative Mössbauer spectra are shown in Figure 5. If it is assumed that the platinum-tin alloy only has the atomic ratio tin:platinum of 1:1, as was found to be the case in X-ray diffraction (XRD) data to be described below, one obtains the results shown in Figure 6. For lower tin to platinum ratios (< 5) little difference is observed in the extent of alloy formation and the distribution of the oxidised species, for a low and high surface area alumina support. In this respect, there is general agreement with data observed in some of the earlier Mössbauer studies. The Mössbauer data in Figure 6 show a similar trend in the extent of alloy formation for the alumina supported

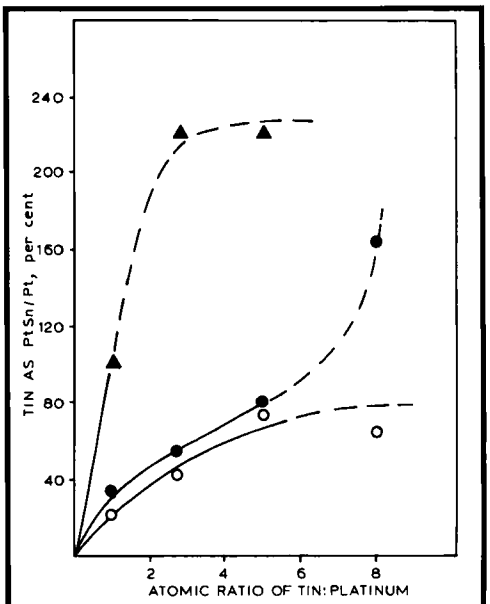

Fig. 6 The amount of tin calculated to be present as Pt-Sn alloy versus Sn:Pt ratio; ▲ silica support; ● low surface area alumina support; ○ high surface area alumina support

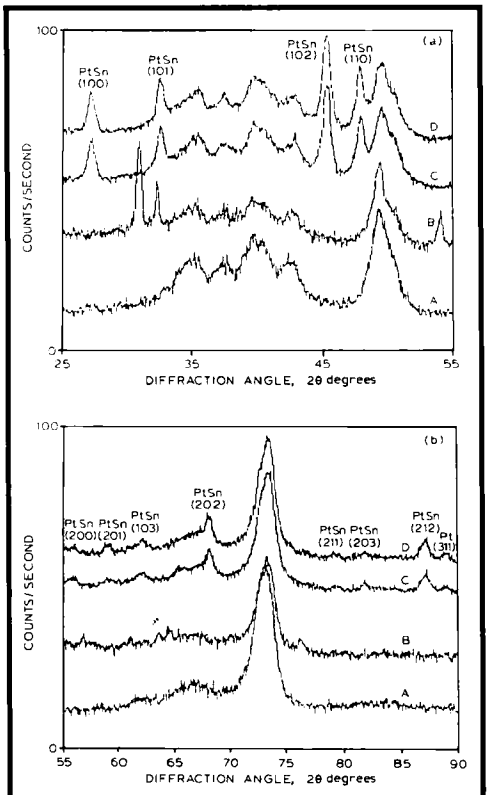

Fig. 7 (a) X-ray diffraction patterns (2 θ = 25 to 55° NiKα radiation for: (A) Degussa alumina catalyst support after calcination for 4 hours at 500°C, (B) 5% Pt prepared from $[Pt_3Sn_8Cl_{20}]^{2-}$ complex after drying at 120°C, (C) sample from B after 8 hours of reduction at 400°C, and (D) sample C after 6 hours of reduction at 550°C. (b) X-ray diffraction patterns (2 θ = 55 to 90°) for samples shown in 7a (see 7a for sample identifications)

materials; the fraction of platinum present in an alloy phase increases with increasing tin concentration and only approaches complete alloy formation at tin:platinum ratio ⩾ about 5.

Platinum-tin supported on silica exhibits much different behaviour than when it is supported on alumina. As reported by others, it is easier to reduce tin to the zero valent state when silica is used as the support (49).

For platinum supported on a co-precipitated tin oxide-alumina catalyst, alloy formation occurs to a much smaller extent than it does on a material prepared by impregnation with the chloride complex (48, 49). Since most commercial catalyst formulations are based on tin/alumina co-precipitated support materials, it appears that the studies using platinum and tin co-impregnation techniques, while interesting, are not directly applicable to the commercial catalysts.

A catalyst was prepared by impregnating a Degussa Aluminium Oxide C (a non-porous alumina of surface area 110 m^2/g) with an acetone solution of $[Pt_3Sn_8Cl_{20}]^{2-}$ (50). A sample of a catalyst containing 5 weight per cent platinum was reduced in situ in the chamber of an XRD instrument; thus the material was not exposed to the atmosphere prior to recording the X-ray diffraction pattern (51). The X-ray diffraction patterns shown in Figure 7 match very well, both in position and intensity, the pattern reported for platinum-tin alloy (Figure 8). In Figure 8, it can be seen that with the 5 weight per cent platinum catalyst, a small fraction of the platinum is present as crystalline platinum but that crystalline platinum was not observed for the 0.6 weight per cent platinum catalyst. It is noted that a similar result for the platinum-tin alloy is obtained for a catalyst that contains only 0.6 weight per cent platinum, with the same tin to platinum ratio. These in situ XRD studies therefore support alloy formation with a stoichiometry ratio of platinum:tin of 1:1. The tin in excess of that needed to form this alloy is present in an X-ray "amorphous" form, and is postulated to be present in a shell layer with a structure similar to that of tin aluminate.

A series of catalysts were prepared to contain 1 weight per cent platinum, and tin to platinum ratios ranging from about 8:1, using a low (110 m^2/g) and high (300 m^2/g) surface area alumina (52). XRD studies indicated that, irrespective of the tin to platinum ratio, the only crystalline phase detected by XRD was platinum-tin (1:1). The XRD intensity of lines for the tin-platinum alloy phase increase with increasing tin to platinum ratios, indicating the presence of unalloyed platinum in the samples containing low tin loadings. The integrated intensity

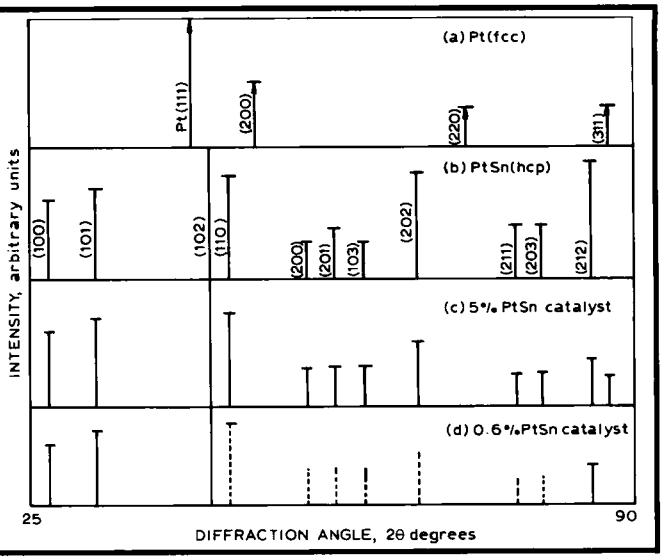

Fig. 8 Diffraction peak positions and relative intensities for (a) Pt (f.c.c.), (b) Pt-Sn (h.c.p.), (c) a reduced Pt-Sn/alumina catalyst with 5 wt. per cent platinum, and (d) reduced Pt-Sn/alumina catalyst with 0.6 wt. per cent platinum

measured for the most intense PtSn peak (102) is plotted versus the tin content on the high and low surface area supports in Figure 9, and clearly shows that the amount of platinum present as crystalline alloy increases with increasing tin:platinum ratios. Also, the crystallite size, calculated from the XRD data, shows that the diameter of the crystallite increases from about 10 to 16 nm with increasing tin content.

X-ray absorption near edge structure (XANES) and extended X-ray absorption fine structure spectra (EXAFS) were obtained for a series of tin-platinum on alumina or silica samples (53, 54). X-ray fluorescence and absorption spectra, at the platinum L_{III}, and tin K-edges, were recorded for dried, calcined and reduced (at 773 K and 1 bar hydrogen) preparations of tin-platinum loaded on silica and alumina supports. The platinum was maintained at 1 weight per cent and the tin content was varied from 0.39 to 3.4 per cent.

The near-edge profiles at the platinum L_{III} and tin K-edges did not show any distinctive features for any of the reference substances or the various catalyst preparations. However, the steep increases in absorption appear at different locations; all edge positions were measured relative to those of the corresponding metal foils, assigned as zero. Typical resolved near-edge profiles are illustrated in Figure 10. The resolved peak height is a measure of its ionicity; that is for platinum the number of 5*d* electrons removed by chemical-bond formation. Horsley showed that the areas of the threshold resonance lines can be estimated by deconvoluting the absorption edge into a Lorentzian

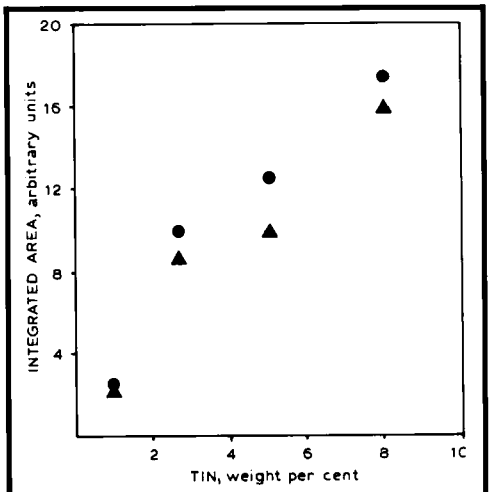

Fig. 9 The integrated intensity measured from the 100% Pt-Sn (102) profile versus Sn content: ● on the United Catalysts, Inc. alumina support and ▲ on Degussa alumina support

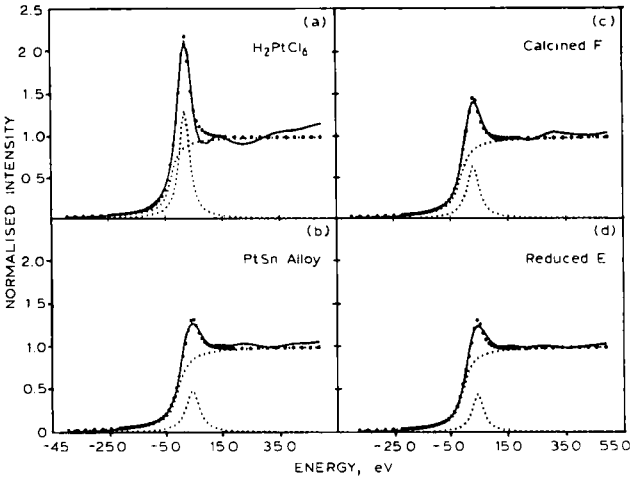

Fig. 10 Profiles at the Pt L_{III} edge, resolved into overlapping Lorentzian and $\tan^{-1}$ functions. The large dots show how well the recorded data (__) are reproduced by the sum (....) of the functions (....)

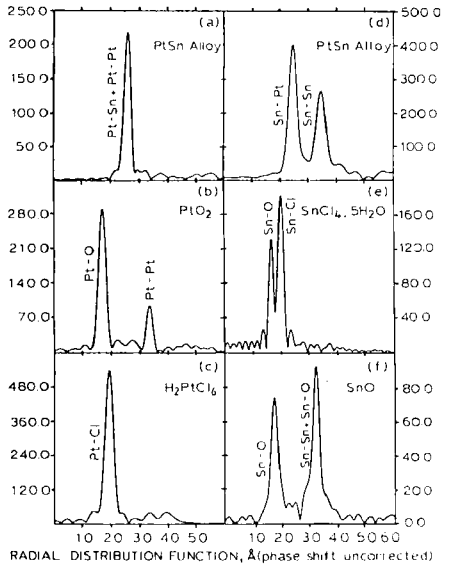

Fig. 11 Radial distribution functions derived for the calibrating materials; (a), (b), (c) at the platinum L_{III} edge, and (d), (e), (f) at the tin K-edge

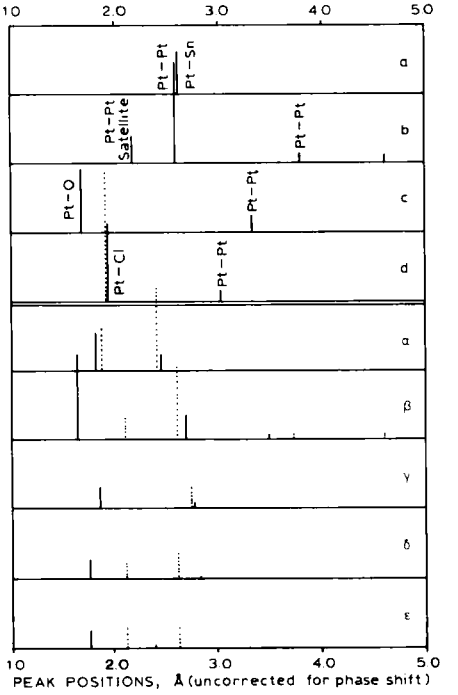

Fig. 12 Peak positions (not corrected for phase shift) are indicated by vertical lines, with approximate peak heights, derived from EXAFS spectra at the Pt L_{III} edge, for several reference compounds and the six catalysts listed in Table II:

(a) Pt-Sn alloy;
(b) Pt metal;
(c) PtO_2;
(d) $PtCl_2 \cdot 2H_2O$ (__) and H_2PtCl_6 (....);
(α) dry preparations: B (__) and F (....);
(β) calcined preparations: B (__) and F (....);
(γ) reduced samples: A (__) and D (....);
(δ) reduced samples: B (__) and E (....);
(ε) reduced samples: C (__) and F (....)

Table II

Catalyst Compositions

Catalyst	Support	Content, weight per cent		
		Platinum	Tin	Chlorine
A	Alumina ~250 m²/g	1.0	0.44	>1.2
B		1.0	1.47	>1.2
C		1.0	3.40	>1.2
D	Silica ~700 m²/g	1.0	0.39	>1.2
E		1.0	0.51	>1.2
F		1.0	0.78	>1.2

component and an underlying "step", which represents the onset of absorption due to a continuum of states (55). In general, it was found that increasing the tin loading on either support decreased the *d* band vacancy for tin. In contrast, alloying platinum with tin leads to an increase in the *d* band vacancies. Overall, alumina favours a higher *d* band vacancy than silica does. These results are in general agreement with those reported by Meitzner and coworkers (49).

The peaks in the radial distribution functions (RDF) for the reference compounds, after background and termination error corrections, provide the basis for assignments of the catalyst RDFs. For reference, RDFs for PtO_2, H_2PtCl_6 and platinum-tin alloy, derived from EXAFS at the platinum L_{III}-edge, and of SnO, $SnCl_4 \cdot 5H_2O$ and the platinum-tin alloy, derived from EXAFS at the tin K-edge, are reproduced in Figure 11. Examination of the RDFs derived from the two sets of scans for the six preparations show both similarities of local structures and striking differences which may be ascribed to control by the supports. In the following text reference will be made to a "stick" diagram (Figure 12), presented to illustrate the distribution of atom-pair distances, plotted as derived, without correcting for phase shifts. A figure of data for the tin K-edge that parallels the data for platinum shown in Figure 12 can be found in Reference 54.

The tin K-edge spectra indicate that the arrangement of atoms about the tin species is essentially the same for both the high area alumina and high area silica supports. Sn-O atom pairs dominate even after reduction, but their contribution decreases somewhat with increasing tin loading. Reference to Figure 12 shows that the two supports lead to a profound difference in configurations of atoms about the platinum. There is a somewhat mysterious 2.5 Å peak in the dried sample for the two supports (spectrum α, Figure 12) and for the reduced sample C (spectrum ε, Figure 12). This peak has been assigned to platinum-tin, as present in the alloy (49).

However, its appearance in the oxidised states of these preparations suggests that a more plausible assumption might be the presence of a solid solution of the oxide, which is incompletely decomposed by calcining or reduction.

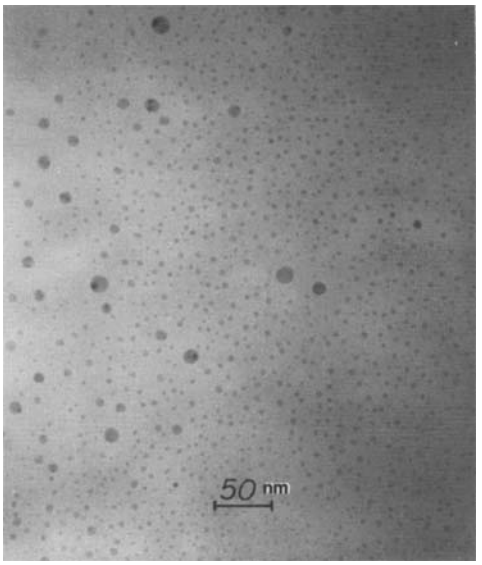

Fig. 13 Representative electron micrograph of a typical co-impregnated Pt-Sn catalyst

An electron microdiffraction technique was employed to identify crystal structures developed in two platinum-tin/alumina catalysts (56). One catalyst was prepared by co-precipitating tin and aluminium oxides and then impregnating the calcined material with chloroplatinic acid to give a platinum:tin atomic ratio of 1:3. The second catalyst was prepared by co-impregnating Degussa alumina with an acetone solution of chloroplatinic acid and stannic chloride to provide a platinum:tin ratio of 1:3. Platinum-tin alloy was not detected by X-ray diffraction for the co-precipitated catalyst although evidence for platinum-tin alloy was found for the co-impregnated catalyst. A representative transmission electron micrograph is shown in Figure 13. Electron microdiffraction studies clearly show evidence for an alloy phase with a platinum:tin ratio of 1:1 in both catalysts. Evidence for minor amounts of alloy with a platinum:tin ratio of 1:2 (for example $PtSn_2$ alloy phase) was also found for the co-precipitated catalyst.

EDX data were obtained for a number of the metal particles present in the two catalysts. The data in Figure 14 represent EDX traces from four small individual particles that are representative of those in the catalyst prepared by co-impregnation with the platinum and tin complex; it is clear that both platinum and tin are observed in each of the particles. Platinum and tin EDX areas were measured for a number of metal particles. The fraction of particles present with various tin:platinum ratios versus the tin:platinum ratio for the co-impregnated catalyst is shown in Figure 15; it is evident that the dominant tin to platinum ratio is 1:1. Considering the uncertainty in the EDX data, it is concluded that the data in Figure 15 are consistent with the finding of an alloy composition of tin:platinum of 1:1, as was obtained by XRD.

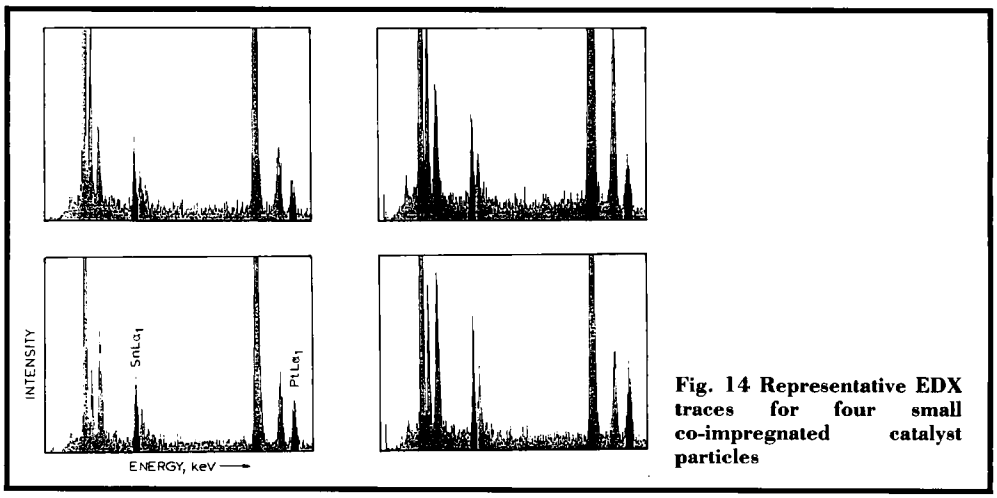

Fig. 14 Representative EDX traces for four small co-impregnated catalyst particles

The EDX data for the co-precipitated tin- and aluminium-oxide give contrasting results. As can be seen in Figure 16, the metal particles large enough for EDX analysis (about 4.0 nm or larger) consist solely of platinum; only rarely is it possible to find a metal particle that contains both platinum and tin. It is therefore concluded that the majority of platinum is present as metallic platinum, and not in an alloy form. As noted above, a few particles were found having a microdiffraction pattern consistent with a platinum:tin ratio of 1:2; it is believed that this composition may be the result of platinum being located on a very few tin rich, or pure tin oxide, regions that were formed during the co-precipitation.

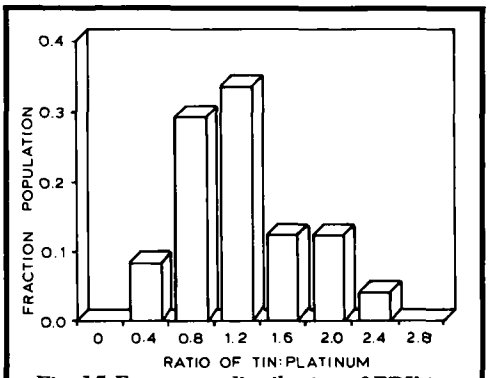

Fig. 15 Frequency distribution of EDX intensity of Sn:Pt ratios for increasing Sn:Pt concentrations

Data from transmission electron microscopy (TEM) show that there are two contrasting structures for alumina supported catalysts of a given tin:platinum chemical composition: one structure is obtained for a co-precipitated material and another for a co-impregnated material. For the co-impregnated material both the tin and platinum are located upon the alumina surface following reduction at about 500°C; the migration of tin or platinum to the bulk does not occur to a measurable extent. Following calcination, most, if not all, of the tin is present in a surface egg-shell layer that chemically resembles a tin aluminate. In forming the tin aluminate some of the tin chloride is converted to a complex that contains more chloride as, for example:

$$2\ SnCl_2 \rightarrow Sn^{2+} + SnCl_4^{2-}$$

Upon reduction some of the tin, if present initially as tin(IV), is converted to tin(II) and tin(0); the fraction of tin that is reduced to tin(0) depends upon the amount of tin in the catalyst. The higher the tin loading, the higher the number of moles (but not necessarily the fraction) of tin that is present in the zero valent state. The amount of platinum-tin alloy will then depend upon the total amount of tin, relative to platinum, that is present in the catalyst; the greater the amount of tin the

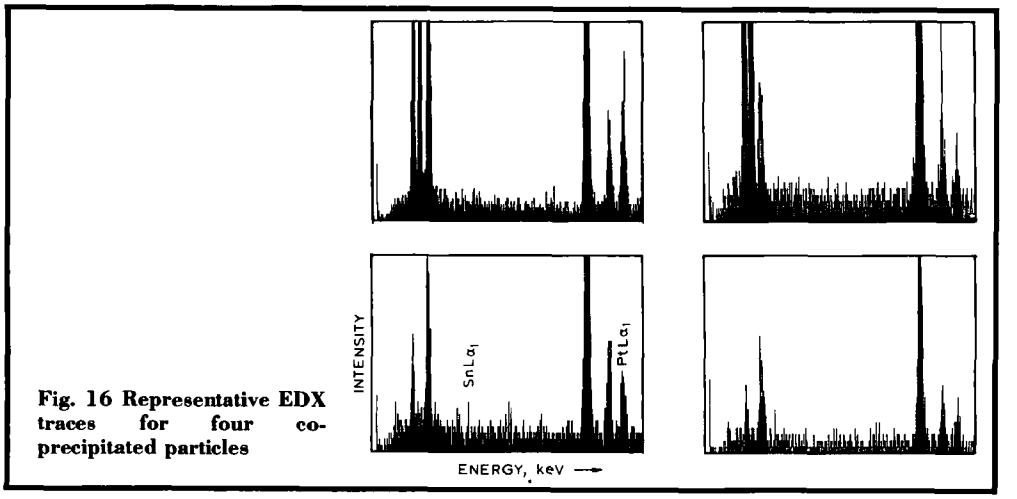

Fig. 16 Representative EDX traces for four co-precipitated particles

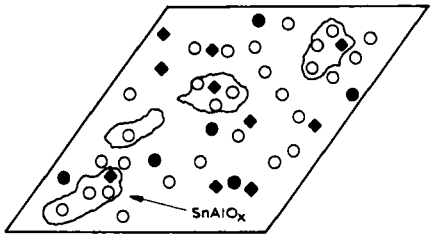

Fig. 17 Schematic of proposed surface structure of a low (1:1) Pt-Sn/alumina catalyst, indicating that most of the platinum present is metallic

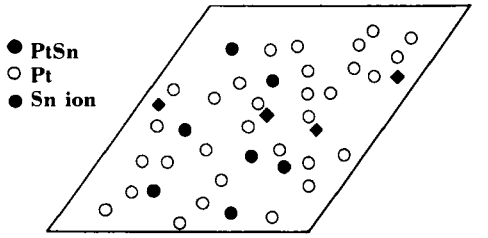

Fig. 18 Schematic of a proposed surface structure of a Pt-Sn catalyst where Pt is impregnated on a co-precipitated tin/alumina (Pt:Sn = 1:3) catalyst

greater the amount of platinum-tin alloy. Thus, we believe that the co-impregnated catalyst consists of chlorostannate complex(es), a surface compound(s) that resembles a tin aluminate, and a mixture of platinum and platinum-tin alloy; the ratio of platinum to platinum-tin alloy will depend upon the composition of the catalyst.

The co-precipitated catalyst differs drastically from that of the co-impregnated catalyst. For the co-precipitated material, a significant, or even a major portion, of the tin will be present in the bulk of the alumina support material; hence, the surface concentration of tin, for a common tin to aluminium ratio, will be much lower for the co-precipitated catalyst. For the co-precipitated material there will be isolated tin ions on the surface of the support; the concentration of these will depend upon the tin to aluminium ratio. Little, if any, of these isolated tin ions will be reduced to the metal; the small amount of tin(0) present is most likely due to the reduction of the few nearly pure tin oxide particles formed during co-precipitation. Upon reduction, nearly all of the platinum will therefore be present as isolated platinum atoms or as platinum metal crystallites. It is postulated that the tin in the co-precipitated material acts as a trap that retards platinum crystal growth, much as was proposed in Reference 4 for another catalyst system.

Thus, we consider the surface of the co-precipitated material to be as shown by the schematics in Figures 17 and 18.

The schematic for a co-impregnated alumina with a low tin to platinum ratio (1:1, in Figure 17) indicates that most of the platinum is present as metallic platinum with some platinum-tin alloy, and that most of the tin is present as the "tin aluminate" compound. For the high tin-platinum co-impregnated catalyst (tin:platinum equals 12:1) a large fraction of the tin can still be regarded as being present as the "tin aluminate" but, because of the larger amount of tin present, sufficient tin(0) is found to convert nearly all of the tin to platinum-tin.

For the co-precipitated catalyst, the schematic representation (Figure 18) indicates that nearly all of the tin on the surface is present as isolated tin(II) — or tin(IV) — ions. The platinum is therefore present as small platinum crystallites. It is speculated that the tin ions serve to "trap" platinum crystallites and retard platinum crystal growth. In this case there should be an optimum where the number of tin ions is about equal to the number of platinum atoms. Thus, the idealised co-precipitated catalyst would consist of isolated tin ion-platinum particles.

The chloride has not been included in the above schematics. The Mössbauer and XPS data indicate that it is likely to be present as $SnCl_4^{2-}$, $SnCl_6^{2-}$ and AlOCl or $AlCl_4$-type complexes. Presumably, these ionic complexes would be highly dispersed both on the surface and in the bulk. The XPS and SEM data clearly indicate that at least a portion of the chloride is mobile during calcination and reduction.

References

1 V. Haensel, "Chemistry of Petroleum Hydrocarbons", eds. B. T. Brooks, C. E. Boord, S. S. Kurtz, Jr. and L. Schmerling, New York, Reinhold, 1955, Vol. 6, p. 189

2 R. L. Jacobsen, H. E. Kluksdahl, C. S. McCoy and R. W. Davis, *Proc. Am. Petr. Inst., Div. Ref.*, 1969, **49**, 504

3 O. Beeck, *Discuss. Faraday Soc.*, 1950, **8**, 118

4 G. B. McVicker, R. L. Garten and R. T. K. Baker, *J. Catal.*, 1978, **54**, 129

5 B. D. McNicol, *J. Catal.*, 1977, **46**, 438

6 V. I. Kuznetsov, E. N. Yurchenko, A. S. Belyi, E. V. Zatolokina, M. A. Smolikov and V. K. Duplakin, *React. Kinet. Catal. Lett.*, 1982, **21**, 419

7 R. Bacaud, P. Bussiere and F. Figueras, *J. Catal.*, 1981, **69**, 399

8 R. Burch, *J. Catal.*, 1981, **71**, 348

9 D. R. Short, S. M. Dhalid, J. R. Katzer and M. J. Kelley, *J. Catal.*, 1981, **72**, 288

10 S. R. Adkins and B. H. Davis, *J. Catal.*, 1984, **89**, 371

11 B. H. Davis, *J. Catal.*, 1977, **46**, 348

12 J. H. Sinfelt, "Bimetallic Catalysis: Discoveries, Concepts, Applications", New York, Wiley, 1983

13 G. Bolivar, M. Charcosset, R. Ferty, M. Primet and L. Tournayan, *J. Catal.*, 1975, **37**, 424

14 N. Wagstaff and R. Prins, *J. Catal.*, 1979, **59**, 434

15 R. Burch, *Platinum Metals Rev.*, 1978, **22**, (2), 57

16 B. A. Sexton, A. E. Hughes and K. Folger, *J. Catal.*, 1984, **88**, 466

17 V. I. Kuznetsov, A. S. Belyi, E. N. Yurchenko, M. D. Smolikov, M. T. Protasova, E. V. Zatolokina and V. K. Duplyakin, *J. Catal.*, 1986, **99**, 159

18 A. C. Müller, P. A. Engelhard and J. E. Weisang, *J. Catal.*, 1979, **56**, 65

19 M. Hansen, "Constitution of Binary Alloys", New York, McGraw-Hill, 1958, p. 1142

20 F. Doerinckel, *Z. Anorg.*, 1907, **54**, 349

21 H. Lieske and J. Völter, *J. Catal.*, 1984, **90**, 46

22 S. R. Adkins and B. H. Davis, "Catalyst Characterization Science", eds. M. L. Deviney and J. L. Gland, ACS Symp. Series, 1985, **22**, 57

23 Y.-X. Li, J. M. Stencel and B. H. Davis, *React. Kinet. Catal. Lett.*, 1988, **37**, 273

24 Y.-X. Li, J. M. Stencel and B. H. Davis, *Appl. Catal.*, 1990, **64**, 71

25 R. Bouwman and P. Biloen, *Surf. Sci.*, 1974, **41**, 348

26 G. B. Hoflund, D. A. Asbury, P. Kirszensztejn and H. A. Laitinen, *Surf. Interface Anal.*, 1986, **9**, 169

27 G. B. Hoflund, "Preparation of Catalysts III", eds. G. Poncelet, P. Grange and P. A. Jacobs, Elsevier, Amsterdam, 1983, pp. 91–100

28 S. D. Gardner, G. B. Hoflund and D. R. Schryer, *J. Catal.*, 1989, **119**, 179

29 D. F. Cox and G. B. Hoflund, *Surf. Sci.*, 1985, **151**, 202

30 S. D. Gardner, G. B. Hoflund, D. R. Schryer and B. T. Upchurch, *J. Phys. Chem.*, 1991, **95**, 835

31 H. A. Laitinen, J. R. Waggoner, C. Y. Chan, P. Kirszensztejn, D. A. Asbury and G. B. Hoflund, *J. Electrochem. Soc.*, 1986, **133**, 1586

32 G. B. Hoflund, D. A. Asbury and R. E. Gilbert, *Thin Solid Films*, 1985, **129**, 139

33 J. M. Stencel, J. Goodman and B. H. Davis, *Proc. 9th Int. Congr. Catal.*, 1988, **3**, 1291

34 V. H. Berndt, H. Mehner, J. Völter and W . Meise., *Z. Anorg. Allg. Chem.*, 1977, **429**, 47

35 R. Bacaud, P. Bussiere, F. Figueras and J. P. Mathieu, *C.R. Acad. Sci. (Paris), Ser. C*, 1975, **281**, 159

36 R. Bacaud, P. Bussiere and F. Figueras, *J. Phys. Colloq.*, 1979, **40**, C2–94

37 J. S. Charlton, M. Cordey-Hayes and I. R. Harris, *J. Less-Common Met.*, 1970, **20**, 105

38 Y.-X. Li, Y.-F. Zhang and K. J. Klabunde, *Langmuir*, 1988, **4**, 385

39 K. J. Klabunde, Y.-X. Li and K. F. Purcell, *Hyperfine Interact.*, 1988, **41**, 649

40 L. Lin, R. Wu, J. Zang and B. Jiang, *Acta Petrol. Sci. (China)*, 1980, **1**, 73

41 N. A. Pakhomov, R. A. Buyanov, E. N. Yurchenko, A. P. Cherynshev, G. R. Kotel'nikov, E. M. Moroz, N. A. Zaitseva and V. A. Patanov, *Kinet. Katal.*, 1981, **22**, 488

42 V.I. Kuznetsov, A.S. Belyi, E.N. Yurchenko, M.D. Smolikov, M. T. Protasova, E. V. Zatolokina and V. K. Duplyakin, *J. Catal.*, 1986, **99**, 159

43 P. R. Gray and F. E. Farha, "Mössbauer Effect Methodology", eds. I. J. Gruverman and C. W. Seidel, Plenum, New York, 1976, Vol. 10, p. 47

44 E. N. Yurchenko, V. I. Kuznetsov, V. P. Melnikova and A. N. Startsev, *React. Kinet. Catal. Lett.*, 1983, **23**, 137

45 P. Zhang, H. Shao, X. Yang and L. Pang, *Cuihua Xuebao*, 1984, **5**, 101

46 Y.-X. Li, Y.-F. Zhang and Y.-F. Shia, *Cuihua Xuebao*, 1984, **5**, 311

47 S. Zhang, B. Xie, P. Wang and J. Zhang, *Cuihua Xuebao*, 1980, **1**, 311

48 Y.-X. Li, K. J. Klabunde and B. H. Davis, *J. Catal.*, 1991, **128**, 1

49 G. Meitzner, G. H. Via, F. W. Lytle, S. C. Fung and J. H. Sinfelt, *J. Phys. Chem.*, 1988, **22**, 2925

50 B. H. Davis, *U.S. Patent* 3,840,475; 1974

51 R. Srinivasan, R. J. De Angelis and B. H. Davis, *J. Catal.*, 1987, **106**, 449

52 R. Srinivasan, R. J. De Angelis and B. H. Davis, *Catal. Lett.*, 1990, **4**, 303

53 Y.-X. Li, N.-S. Chiu, W.-H. Lee, S. H. Bauer and B. H. Davis, "Characterization and Catalyst Development. An Interactive Approach", ACS Symp. Series, 1989, **411**, 328

54 N.-S. Chiu, W.-H. Lee, Y.-X. Li, S. H. Bauer and B. H. Davis, "Advances in Hydrotreating Catalysts", eds. M. L. Occelli and R. G. Anthony, Elsevier, Amsterdam, 1989, pp. 147–163

55 J. A. Horsley, *J. Chem. Phys.*, 1982, **76**, 1451

56 R. Srinivasan, L. A. Rice and B. H. Davis, *J. Catal.*, 1991, **129**, 257